

Texture Formation in Aluminum Solid Solution Alloys by High-temperature Deformation

Hiroshi Fukutomi and Kazuto Okayasu

Department of Solid State Materials and Engineering,
Graduate School of Yokohama National University
79-5 Tokiwadai Hodogaya-ku Yokohama 240-8501, Japan

The effect of high temperature deformation on the texture formation is experimentally examined on Al-Mg, Al-Cu and commercial Al alloys by uniaxial compression deformation. When atmosphere dragging dominates the high temperature deformation, texture transition with increasing strain from $\{011\}$ (compression plane) to $\{001\}$ fiber texture occurs. It was found that the transition was delayed in Al-3Mg-0.2Sc with Al_3Sc precipitates, suggesting that the formation of $\{001\}$ texture could be attributed to grain boundary migration. It is concluded that the orientation stability for deformation as well as the dislocation structure reflecting the deformation mechanism plays an important role in the development of $\{001\}$ texture after the formation of $\{011\}$ texture.

Keywords: *high temperature deformation, solid solution, solute atmosphere, dislocation structure*

1. Introduction

Texture has strong effects on the mechanical properties of polycrystalline metals and alloys. For example, the development of $\{111\}$ texture contributes to improve deep drawability of aluminum alloys through the increase in r-value [1]. Thus it is important to understand the mechanism of texture evolution and find new methods to control textures. Usually, textures in metals and alloys are controlled by the deformation at room temperature or the combination of deformation at room temperature and heat treatments for recrystallization. In these cases, deformation has two roles: crystal rotation due to crystal slip and the generation of stored energy necessary for recrystallization.

In the case of high temperature deformation of solid solution alloys, it was found that dislocation structure varied depending on deformation mechanism, which could be controlled by deformation conditions. The change in dislocation structure results in the changes of the amount and the spatial distribution of stored energy during deformation. It is also expected that the orientation dependence of the stored energy might be changed. Thus it was considered that the texture changed depending on temperature, strain rate, and the amount of strain at high temperature deformation. The authors investigated the formation behavior of textures in Al-Mg solid solution during high temperature deformation [2]. In this study, the relationship between deformation conditions of uniaxial compression and texture formation is given on Al-Mg, Al-Cu and two commercial Al alloys, AA5052 and AA5182 [3, 4].

2. Experimental Procedure

Al-3, 5, and 10mass%Mg (hereafter described as Al-3Mg, Al-5Mg, and Al-10Mg) and Al-4.6mass%Cu (hereafter described as Al-4.6Cu) alloys were produced by casting. For comparison with Al-3Mg, Al-3mass%Mg-0.2mass%Sc (hereafter described as Al-3Mg-0.2Sc) alloy was prepared. Al-3Mg-0.2Sc was solution treated at 873K for 1hr followed by the aging at 773K for 49hrs. Microstructure observation showed that Al_3Sc precipitates were formed at grain boundaries by the aging. After homogenization, the ingots of these alloys were cold rolled. Cylindrical specimens with the aspect ratio of 1.5 were taken out by spark erosion technique from the cold rolled plates for uniaxial compression deformation. Before compression deformation, final annealing was conducted. Deformation was performed at the temperatures achieving the single phase state under the strain rates

ranging from $1.0 \times 10^{-4} \text{ s}^{-1} \sim 5.0 \times 10^{-2} \text{ s}^{-1}$ up to the true strains in the range between -0.3 and -1.7. After the deformation, the specimens were quenched into water to avoid the microstructure from changing after deformation. The mid-plane sections of the deformed specimens were taken out for texture measurements by mechanical and electrolytic polishing. Textures were measured by the Schulz reflection method using nickel filtered Cu K_{α} radiation. $\{111\}$, $\{110\}$, and $\{001\}$ pole figures were evaluated. Based on these pole figures, orientation distribution function (ODF) was calculated by the Dahms-Bunge method [5]. Based on the ODF, inverse pole figures were derived. For evaluating the local distribution of crystal orientations and the microstructure observation, SEM equipped with EBSD system was used.

3. Results and discussion

3.1 Deformation behavior

Figure 1 shows the true stress-true strain curves for Al-3Mg and Al-4.6Cu. Due to the difference in the temperature range of single phase region, the deformation is conducted at 723K for Al-3Mg and at 803K for Al-4.6Cu. The stress-strain curves show the peak in true stress at the beginning of deformation. This is the so-called high temperature yielding [6]. Stress-strain curves with high temperature yielding were seen also in the compression deformation of AA5052 and AA5182 alloys. It was seen that flow stresses increased with decreasing temperature and increasing strain rates. Figure 2 is the double logarithmic plot of flow stresses at a strain of -0.5 against strain rates for Al-3Mg. Linear relationship holds between strain rates and flow stresses. The slope of the line is about 3 which coincides with the experimental results reported previously [7,8]. Horiuchi and Otsuka clarified that so called atmosphere dragging dominated the deformation in this case [7].

3.2 Texture

Figure 3 shows the $\{011\}$ pole figures examined on (a) Al-3Mg, (b) Al-5Mg, and (c) Al-10Mg alloys after the deformation up to a strain of -1.0 at 723K with a strain rate of $5.0 \times 10^{-4} \text{ s}^{-1}$. Pole densities are projected onto the compression plane and the mean pole density is used as a unit for drawing the contours. In all pole figures, the pole densities are distributed in a concentric circular manner, indicating the formation of fiber textures. The circles in the pole figure correspond to 45 and 60 degrees from the center. Area of high pole density appears in the center and the region between 45 and 60 degrees from the center in Fig. 3(a), while no pole densities are seen in the center of Fig. 3 (b) and (c). This means that the texture components are different among these three alloys. In order to specify the texture components for Fig. 3(a), (b), and (c), inverse pole

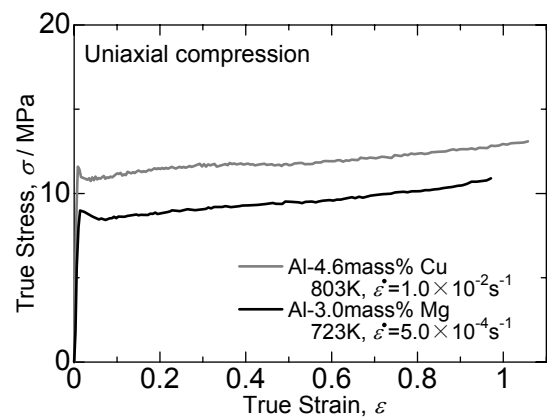


Fig. 1 True stress-true strain curves of Al-3Mg and Al-4.6Cu alloys. Deformation conditions for Al-3Mg and Al-4.6Cu are at 723K with a strain rate of $5.0 \times 10^{-4} \text{ s}^{-1}$ and at 803K with a strain rate of $1.0 \times 10^{-2} \text{ s}^{-1}$, respectively.

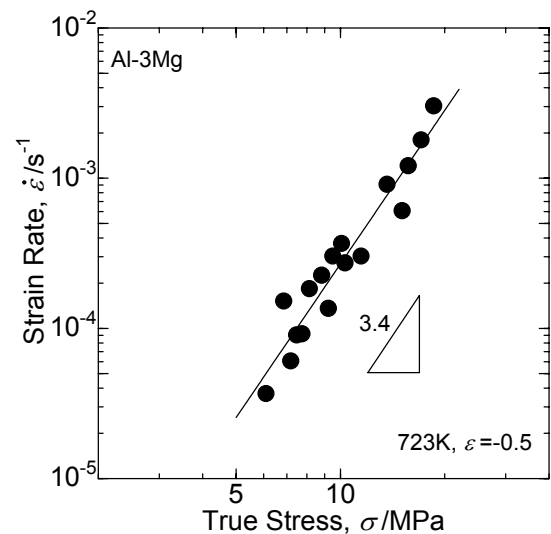


Fig. 2 True stress vs. strain rate relationship for Al-3Mg examined at a strain of -0.5. The deformation is conducted at 723K.

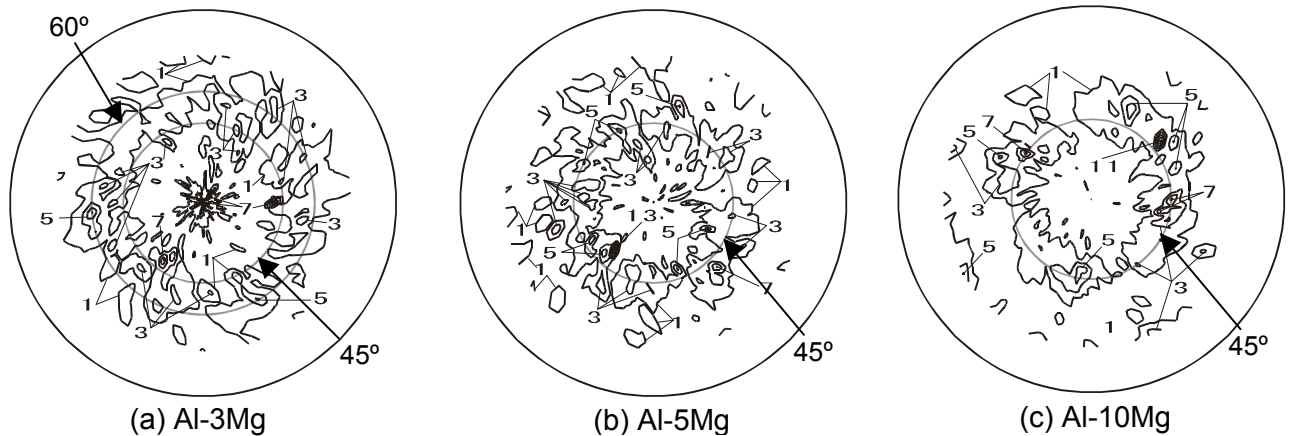


Fig. 3 $\{011\}$ pole figures for (a) Al-3Mg, (b) Al-5Mg, and (c) Al-10Mg alloys after the deformation up to a strain of -1.0 at 723K with a strain rate of $5.0 \times 10^{-4} \text{s}^{-1}$. Pole densities are projected onto the compression plane. Mean pole density is used as a unit for drawing the contours.

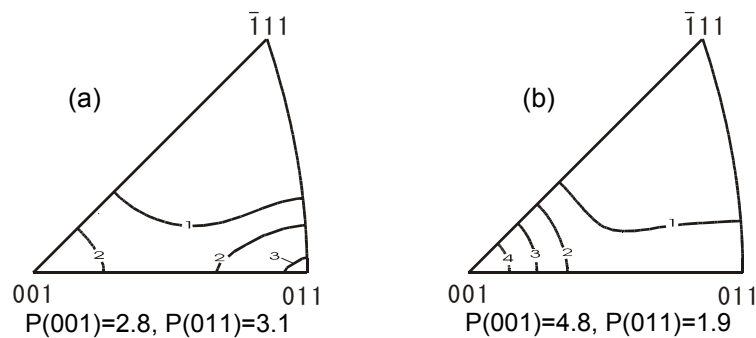


Fig. 4 Inverse pole figures showing the effect of strain on the components of the fiber texture constructed in Al-3Mg. The deformation was conducted at 723K with a strain rate of $5.0 \times 10^{-4} \text{s}^{-1}$. The amounts of strain are (a) -1.0 and (b) -1.4 . Contour lines for the densities of compression axis are given. Mean density is used as a unit. $P(001)$ and $P(011)$ express the pole density at (001) and (011) , respectively.

figures were examined. It was found that $\{011\} + \{001\}$ fiber texture was formed in Al-3Mg and $\{001\}$ fiber texture developed in Al-5Mg and Al-10Mg alloys at this deformation condition. Furthermore, it was found that the change in the main component did not depend on the solute contents but the amount of strain in these alloys.

Figure 4 (a) and (b) show the effect of strain on the main component of the fiber texture. The results of texture measurements after the deformation up to strains of (a) -1.0 and (b) -1.4 under the strain rate of $5.0 \times 10^{-4} \text{s}^{-1}$ at 723K are given. In Fig. 4(a), there are two areas of high pole density with different densities; the main component is (011) . At a strain of -1.4 , the pole density at (001) increases up to 4.8 , while the density at (011) is 1.9 . This indicates that (001) component develops by consuming (011) texture component.

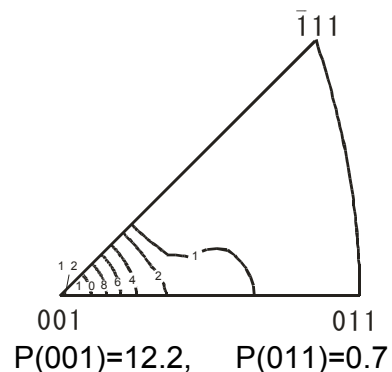


Fig. 5 Development of $\{001\}$ fiber texture in Al-4.6Cu by the deformation at 803K with a strain rate of $5.0 \times 10^{-3} \text{s}^{-1}$ up to a strain of -1.0 .

Figure 5 is the result of Al-4.6Cu which is deformed at 803K up to a strain of -1.0. The strain rate is $5.0 \times 10^{-3} \text{ s}^{-1}$. The pole density at (001) is quite high such as 12.2 and the pole density at (011) is below unity. The formation of {001} fiber texture after the development of {011} texture was also found in the commercial aluminum alloys, AA5182 and AA5052 [4].

3.3 Effect of grain boundary migration on the development of {001} with increasing strain

In order to examine the mechanism of texture change from {011} to {001} with increasing strain, the behavior of texture formation and the microstructure evolution by high temperature deformation are investigated on Al-3Mg-0.2Sc alloy with Al_3Sc precipitates. Figure 6 shows the inverse pole figures for the compression plane after the deformation at 723K under a strain rate of $5.0 \times 10^{-4} \text{ s}^{-1}$ up to a strain of -1.0 for (a) Al-3Mg and (b) Al-3Mg-0.2Sc.

In both inverse pole figures, pole densities are high at (001) and (011). In the case of Al-3Mg binary alloy, the pole density at (001) is 2.8 which is higher than that for Al-3Mg-0.2Sc alloy while in the case of (011), the pole density of Al-3Mg binary alloy is lower than that of Al-3Mg-0.2Sc. Namely, the development of {001} texture is delayed in Al-3Mg-0.2Sc alloy.

Figure 7 shows the microstructures observed at the cross sections of (a) Al-3Mg-0.2Sc and (b) Al-10Mg after the high temperature deformation. Compression deformation was made from the top and bottom directions. The deformation was conducted at 723K with a strain rate of $5.0 \times 10^{-4} \text{ s}^{-1}$ up to -1.0 in true strain. Although the deformation condition is the same, difference is seen obviously in the microstructures. In the case of Al-3Mg-0.2Sc, the grains are platelet shape, while equiaxed microstructure is constructed in Al-10Mg. The intermediate state appeared in Al-3Mg. Furthermore, it was found that the frequency of crystal grains with the orientation close to {001} was high in Al-10Mg in comparison with Al-3Mg. These characteristics of the microstructure suggest that the development of {001} texture can be

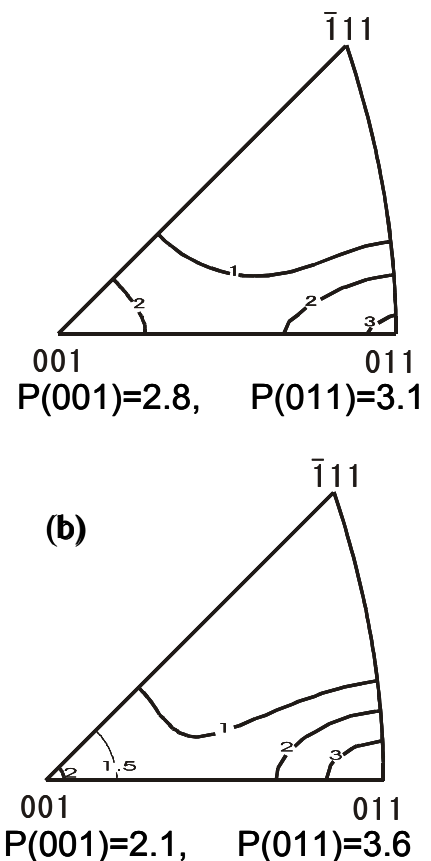


Fig. 6 Inverse pole figures for the compression plane after the deformation at 723K up to a strain of -1.0. (a) Al-3Mg and (b) Al-3Mg-0.2Sc [2].

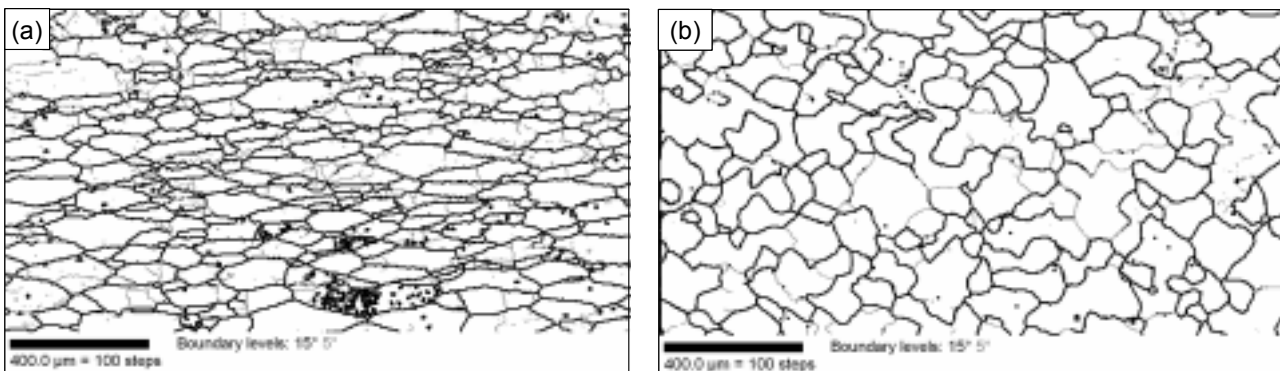


Fig. 7 Microstructures observed at the cross section after the deformation at 723K with a strain rate of $5.0 \times 10^{-4} \text{ s}^{-1}$ up to -1.0 in true strain. (a) Al-3Mg-0.2Sc and (b) Al-10Mg. Thick and thin lines express the high angle grain boundaries with the misorientations higher than 15 degrees and low angle grain boundaries, respectively.

attributed to the preferential migration of the grain boundaries surrounding the grains with $\{001\}$ orientation.

3.4 Mechanism of the development of $\{001\}$ fiber texture

Crystal slip deformation generates the deformation texture. It is known that the uniaxial compression deformation of FCC crystals develops the $\{011\}$ (compression plane) texture when $\{111\}\langle 011\rangle$ slip system works. The major slip system of Al-Mg alloys at high temperatures is $\{111\}\langle 011\rangle$ and hence the formation of $\{011\}$ texture can be understood as a usual behavior of texture formation in FCC crystals. The development of $\{001\}$, however, has been seldom reported. Stout *et al.* [9] found the formation of $\{011\} + \{001\}$ texture by a uniaxial compression. They reported that the formation of $\{001\}$ could not be explained by the static recrystallization and proposed that the formation of $\{001\}$ texture might be attributed to the activation of slip systems other than $\{111\}\langle 011\rangle$ based on the texture simulation.

The effect of strain on the development of $\{001\}$ texture given in Fig. 4 and the microstructure observation given in Fig. 7 suggest another possibility, which is mentioned in 3.3; the effect of grain boundary migration.

As shown in Fig. 4, $\{011\}$ texture develops at the initial stage of deformation. This can be understood as the result of $\{111\}\langle 011\rangle$ slip. During the deformation, dislocations are multiplied and dislocation structure develops. Horiuchi and Otsuka [7] showed that dislocations did not form subgrains but were distributed uniformly due to the effect of solute atmosphere. In this case, it is expected that the orientation dependence of stored energy is enhanced in comparison with the uneven distribution of dislocations. It is considered that the grains with orientations having low Taylor factor might have lower stored energy than other grains with higher Taylor factor and grow during the high temperature deformation. Taylor factor for $\{011\}$ and $\{001\}$ was reported as 3.674 and 2.449, respectively [10]. This difference in Taylor factor is consistent with the observed change in the main component of the texture with increasing strain.

The minimum value of Taylor factor for the axisymmetric flow of FCC crystals with $\{111\}\langle 110\rangle$ slip system is 2.3 at the orientation about 10 degrees far from $\{001\}$ along the great circle connecting $\{001\}$ and $\{111\}$. This means that the development of $\{001\}$ can not be explained only by the viewpoint of stored energy. Here, it should be noted that $\{001\}$ is formed during deformation. Since the stable orientation for uniaxial compression is $\{011\}$, the crystal slip drives the grains with orientations different from $\{011\}$ to the stable orientations, namely, $\{011\}$. However, orientations with high symmetry are insensitive to the lattice rotation because of a multiple slip. In the case of $\{001\}$, eight equivalent slip systems can contribute to the axisymmetric flow, which makes it possible to survive from the large crystal rotation. Thus it is considered that the development of $\{001\}$ can be attributed to the low stored energy and orientation stability.

3.5 Effect of deformation mechanism on the development of $\{001\}$ texture

Deformation mechanisms vary depending on deformation conditions at high temperatures [11]. Figure 4 shows that the $\{001\}$ texture sharpened with increasing strain. The sharpening with increasing strain is observed in Al-Mg, Al-Cu, AA5052, and AA5182 in general. However, in some cases, it was found that the further deformation by the constant crosshead speed mode resulted in the deceleration of the $\{001\}$ texture sharpening. Examination of the deformation mechanism map of Al-4.6Cu [11] suggested that the increase in the strain rate with increasing strain might change the dominant deformation mechanism of this alloy which resulted in the formation of subgrains after large amount of deformation.

In order to examine the relationship between the deformation mechanism and the $\{001\}$ texture development in such case, strain rate was decreased after the certain amount of deformation and the textures were evaluated. It was found that texture sharpening was accelerated by the change in the strain rate, coinciding with the consideration that the dislocation distribution is one of the key factors

dominating the {001} texture development. For understanding the effects of temperature and strain rate on the development of {001} texture, {001} texture map is constructed on AA5182 and AA5052 [3, 4] alloys. The map suggests that sharpness of {001} texture varies depending on strain rate and deformation temperature.

4. Conclusions

The characteristics of texture formation in Al solid solution alloys during high temperature deformation are experimentally studied by uniaxial compression deformation. It was found that texture developed with increasing strain when atmosphere dragging dominated the deformation. In this case, {011} (compression plane) fiber texture was formed at the early stage of deformation, followed by the development of {001} fiber texture. This behavior was experimentally confirmed on Al-Mg, Al-Cu and two kinds of commercial aluminum alloys, AA5052 and AA5182. It was shown that the basic process for {001} texture formation is the grain boundary migration driven by the difference in the stored energy of crystal grains. It was concluded that the development of {001} texture could be attributed to the relatively low stored energy which originated from the dislocation structure and low value of Taylor factor of this orientation, and the stability for uniaxial compression deformation.

Acknowledgements

The authors greatly acknowledge the financial support of the Japan Light Metal Foundation. The authors also appreciate Mr. M. Kinoshita, Mr. S. Takahata, Miss H. Shimada, Mr. M. Sakakibara and Mr. H. M. Jeong for their help in performing various kinds of experiments.

References

- [1] H. Inoue and T. Takasugi: Mater. Trans. 48 (2007) 2014–2022.
- [2] K. Okayasu, H. Takekoshi and H. Fukutomi: Mat. Trans. 48 (2007) 2002-2007.
- [3] H. M. Jeong, K. Okayasu and H. Fukutomi: submitted to Mater. Trans. (2010).
- [4] H. M. Jeong, K. Okayasu and H. Fukutomi: Proc. ICAA12 (2010).
- [5] M. Dahms and H. J. Bunge: J. Appl. Crystallogr. 22 (1989) 439-447.
- [6] R. Horiuchi, H. Yoshinaga and S. Hama: J. Japan Inst. Metals 29 (1965) 85-92.
- [7] R. Horiuchi and M. Otsuka: J. Japan Inst. Metals 35 (1971) 406-415.
- [8] H. Oikawa, J. Kariya and S. Karashima: Met. Sci. 8 (1974) 106-111.
- [9] M. G. Stout, S. R. Chen, U. F. Kocks, A. J. Schwartz, S. R. MacEwen, and A. J. Beaudoin: *Hot Deformation of Aluminum Alloys II*, Ed. by T. R. Bieler, L. A. Lalli, and S. R. MacEwen, (The Minerals, Metals and Materials Society, 1998) pp. 243-254.
- [10] G. Y. Chin and W. L. Mammel: Trans. Metall. AIME 239 (1967) 1400-1405.
- [11] T. Ito, M. Ishikawa and M. Otsuka: J. Japan Inst. Metals 66 (2002) 832-839.